

## Synthesis and optical properties of zinc phosphate microspheres

Zhang-lei NING, Wen-jun LI, Chang-yan SUN, Ping CHE, Zhi-dong CHANG

School of Chemical and Biological Engineering, University of Science and Technology Beijing, Beijing 100083, China

Received 15 May 2012; accepted 8 October 2012

**Abstract:** Monodisperse zinc phosphate microspheres were synthesized by a facile solvothermal method in the presence of oleic acid. X-ray powder diffraction (XRD), Fourier transform infrared spectrum (FT-IR), emission scanning electron microscopy (SEM), and energy dispersive X-ray spectrum (EDX) were used to characterize the microstructures and morphologies of the as-obtained zinc phosphate samples. The experimental results indicate that the zinc phosphate products are well crystallized, and the morphologies of the samples can be easily controlled by the elaborate choice of oleic acid addition and the content of NaOH. Furthermore, self-activated luminescent properties of the products are observed. The as-obtained samples show an intense blue emission under a long-wavelength UV light excitation of 400 nm. The possible luminescent mechanism may be ascribed to the carbon-related surface impurities or defects.

**Key words:** zinc phosphate; oleic acid; chemical synthesis; optical properties; luminescence

### 1 Introduction

In the past decades, the synthesis of nano- and micro-crystals with controllable morphology and architecture has attracted much attention in material chemistry, because it is well-known that the properties of the materials closely interrelate with their geometrical factors such as the size, shape, and dimensionality [1]. The introduction of surfactants in the synthesis process has been proven to be an efficient and promising way to control the shape and morphology of the materials. The surfactant not only provides favorable site for the growth of the particulate assemblies, but also influences the formation progress, including the nucleation, growth and coagulation. Recently, many materials have been used as surfactants including cetyltrimethyl ammonium bromide (CTAB) [2], polyvinylpyrrolidone (PVP) [3] and oleic acid [4,5].

Inorganic luminescent materials have been widely used in fluorescent lamps, light emitting displays, cathode-ray tubes and white light emitting diodes (LEDs) [6–8]. Among the family of inorganic luminescent compounds, zinc phosphate ( $Zn_3(PO_4)_2$ ) is one kind of commonly used luminescent host material. For example, zinc phosphate powders doped with  $Mn^{2+}$  are efficient

red long-lasting phosphorescent materials [9,10]. Silver zinc phosphates exhibit luminescence properties in the visible spectral range [11]. Zinc phosphate doped or co-doped with rare earth metal such as  $Eu^{3+}$  [12–14],  $Tb^{3+}$  [15] and  $Tm^{3+}$  [16] shows excellent luminescent properties. However, most of them are doped with luminescent centers and excited by short-wavelength ultraviolet (UV) light for the operation. The luminescent centers such as rare earth elements (RE) or silver are typically expensive. In addition, the use of mercury vapor plasma for the production of the short-wavelength UV will cause environmental contamination [17,18]. Therefore, much effort has been devoted to exploring self-activated luminescent materials that do not contain expensive elements or can be excited by long-wavelength UV light. Up to now, only a few examples have been reported about the self-activated luminescent inorganic materials including  $SrCO_3$  [17,19],  $SiO_2$  [20],  $NaMgF_3$  [21] and  $Y_2O_3$  [22]. However, to the best of our knowledge, there is no report about the self-activated luminescent zinc phosphate.

Herein, monodisperse zinc phosphate microspheres were synthesized by a facile solvothermal method. The influences of the synthetic parameters on the morphologies of the final products were investigated. Moreover, the photoluminescent properties of zinc

phosphate were also studied, which revealed a novel self-activated luminescent phenomenon.

## 2 Experimental

### 2.1 Materials and preparation

All chemicals were analytically pure and were used without further purification. In a typical procedure, oleic acid (3.5 mL), ethanol (15 mL) and a certain amount of sodium hydroxide (NaOH) were mixed together. And 8 mL  $Zn(NO_3)_2$  (1.875 mmol/L) and 8 mL  $(NH_4)_2HPO_4$  (1.25 mmol/L) aqueous solution were added to the above solution in sequence under vigorous stirring. Then, the solution was transferred into a 50 mL stainless-steel autoclave, sealed and treated at 180 °C for 24 h. After cooling to room temperature naturally, the products were obtained by centrifugation, washed with deionized water and absolute alcohol in order, and then dried at 60 °C for 24 h.

### 2.2 Characterization

X-ray powder diffraction (XRD) test was performed on a D/MAX-RB diffractometer (Rigaku, Japan) with Cu  $K_\alpha$  source ( $\lambda=0.15405$  nm) in the  $2\theta$  range from 10° to 70°. The Fourier transform infrared (FT-IR) spectrum was obtained on an NEXUS 670 infrared spectrophotometer (Thermo Nicolet, US) with KBr tablets. The morphology was observed via a Quanta 450 emission scanning electron microscope (SEM) (FEI, US) and imaged without carbon sputtering. The energy dispersive X-ray spectrum (EDX) was measured with an XFlash 5010 detector (Bruker, Germany). The photoluminescence (PL) emission and excitation spectra were measured on an F-4500 fluorescence spectrophotometer (Hitachi, Japan) equipped with a 150 W xenon lamp as the excitation source. The decay curve was recorded with the Edinburgh analytical instruments F-900 (Edinburgh Instruments Ltd., UK). All the measurements were performed at room temperature.

## 3 Results and discussion

### 3.1 XRD and FT-IR analysis

In order to identify the phase composition of the products, X-ray diffraction (XRD) was employed (Fig. 1). The strong and narrow peaks indicate that the as-prepared samples are well-crystallized in spite of the moderate reaction condition. All the diffraction peaks of the sample coincide well with the standard data of zinc phosphate hydrate ( $Zn_3(PO_4)_2 \cdot xH_2O$ ,  $x=2, 4$ ) (JCPDS 33-1474, 37-0316 and 37-0465). No other phases can be detected in the XRD pattern, indicating that zinc phosphate crystals have been obtained by this method. There are several zinc phosphate hydrates coexisting

in the as-obtained samples, similar to that reported in Ref. [23].

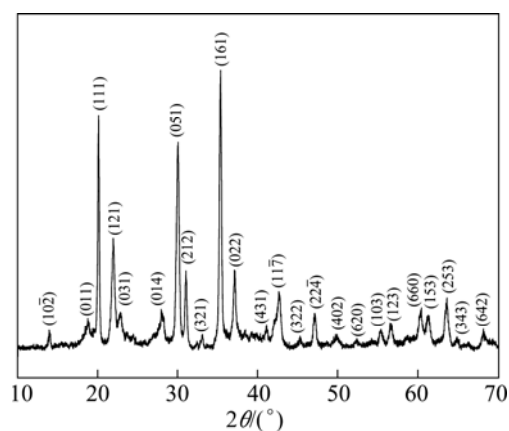


Fig. 1 XRD pattern of as-prepared zinc phosphate microspheres

Figure 2 illustrates the FT-IR spectrum of the as-obtained samples. A set of characteristic peaks at 1092, 1025, 636, 606, 556 and 510  $cm^{-1}$  are attributed to the complex stretching and bending vibrations of the  $PO_4^{3-}$  group. The peak at 1640  $cm^{-1}$  and a broad band centered at about 3422  $cm^{-1}$  are assigned to —OH bending and stretching vibration, respectively. The additional peaks at 2969, 2924, and 2846  $cm^{-1}$  are ascribed to the symmetric and antisymmetric stretch vibration of the — $CH_2$  group, indicating the existence of the organics within the particles even if they have been washed by deionized water and alcohol. The band of C=O at 1710  $cm^{-1}$  of the nonionized carboxyl group of the pure oleic acid disappears [24], but a new band appears at 1445  $cm^{-1}$ , which corresponds to the coordination of  $COO^-$  with  $Zn^{2+}$  [21,25]. So it can be concluded that a certain level of carbon-related impurities exist in the zinc phosphate products [26,27].

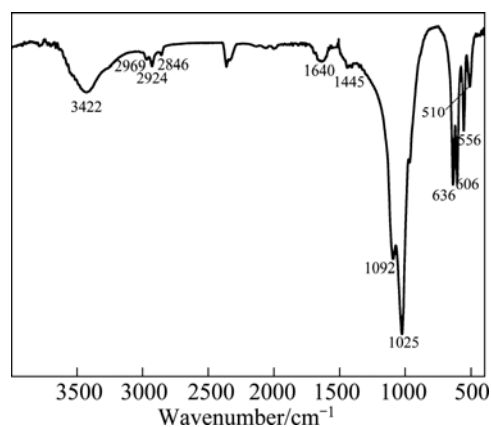


Fig. 2 FT-IR spectrum of zinc phosphate microspheres

### 3.2 Influences of different reaction parameters on morphology of zinc phosphate samples

Different reaction parameters were selected to

investigate the morphology and understand the growth process of zinc phosphate products. Scanning electron microscopy (SEM) was used to determine the morphology of the as-prepared samples.

### 3.2.1 Effect of oleic acid on morphology

A control experiment was carried out in the absence of oleic acid with other parameters constant. The typical SEM images of the samples synthesized without and with oleic acid are presented in Fig. 3. In the absence of oleic acid, the morphologies of the as-prepared samples are amorphous agglomerated nanoparticles (Fig. 3(a)). While with oleic acid, the products are almost entirely composed of microspheres with perfect monodispersity (Fig. 3(b)). This demonstrates that oleic acid plays an important role in the formation of sphere-shaped zinc phosphate products. Oleic acid, as a surfactant with a long alkyl chain, can be adsorbed on the crystal surfaces of the products and act as an efficient capping reagent to control the growth of the products. Some studies have been reported for the high performance of oleic acid in producing inorganic materials with well-controlled morphology such as spike-like  $\text{CaCO}_3$  [28], colloidal orthovanadate nanocrystals [29] and monodisperse iron oxide [30].

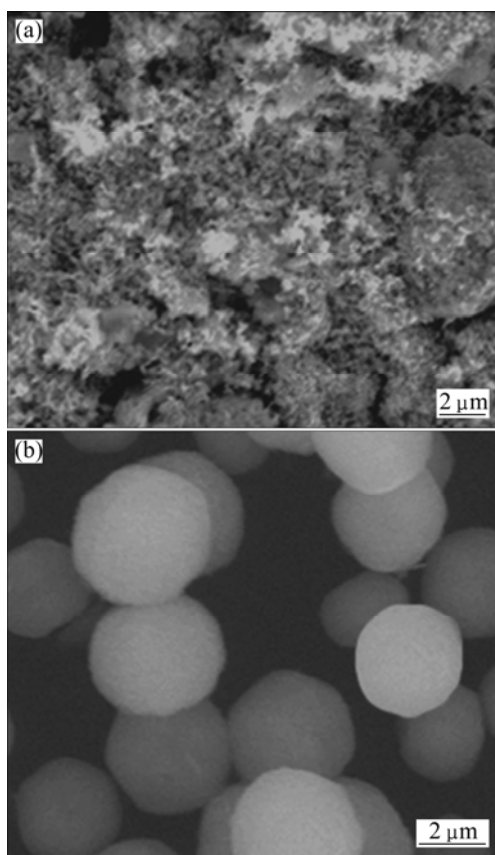
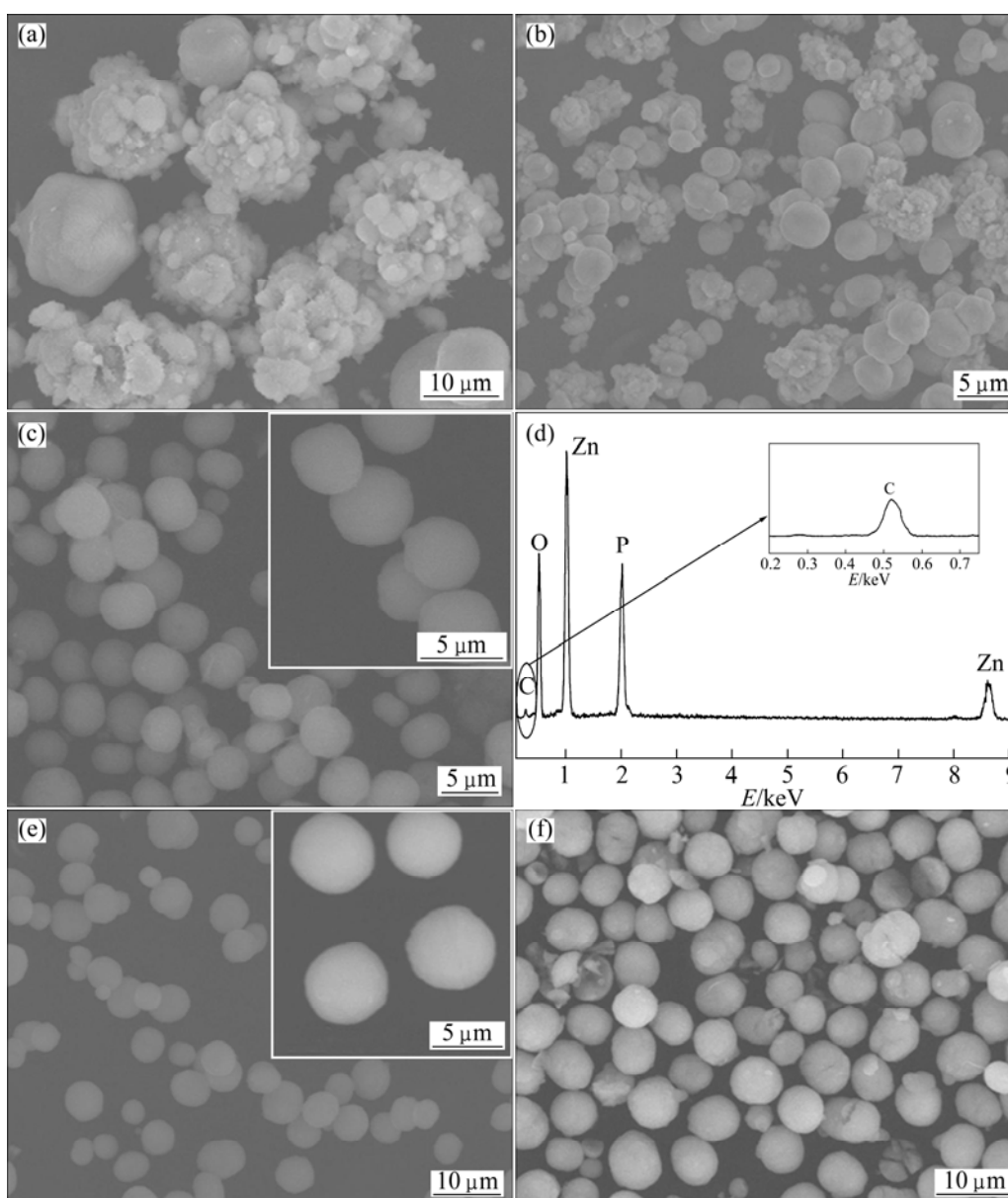


**Fig. 3** SEM images of as-obtained zinc phosphate products synthesized with 0.30 g NaOH: (a) Without oleic acid; (b) With oleic acid

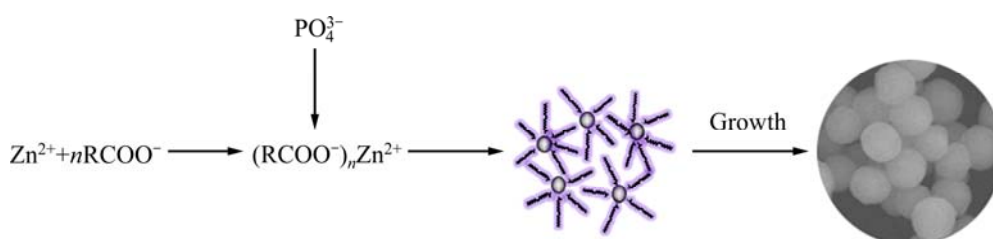
### 3.2.2 Effect of NaOH addition

Figure 4 illustrates SEM images of the as-prepared samples with different contents of NaOH from 0.20 to 0.45 g with other parameters constant. When the content of NaOH is 0.20 g, the as-prepared samples are agglomerations consisting of irregular sphere and amorphous particles (Fig. 4(a)). By increasing the NaOH addition to 0.25 g, the agglomerations change into small pieces and some spherical particles appear (Fig. 4(b)). When the content of NaOH reaches 0.30 g, the as-prepared samples are monodisperse microspheres with uniform size in the range of 3–5  $\mu\text{m}$  (Fig. 4(c)). The EDX spectrum (Fig. 4(d)) of zinc phosphate shows the presence of Zn, P, O and C. The similar situation holds for other samples. The detected carbon (also observed in the FT-IR spectrum) indicates that some carbon impurities have been induced into the host lattices and/or the surface. Further increasing the NaOH content to 0.40 g, there are no further changes in the sphere-shape, but the size increases to about 5–8  $\mu\text{m}$  (inset in Fig. 4(e)). When the content of NaOH increases to 0.45 g (Fig. 4(f)), the spheres become deformed and some of them are broken. These results indicate that NaOH also has an obvious effect on the formation of the sphere-shaped particles.

In the synthesis process, liquid-solid-solution (LSS) strategy was employed, which designs the chemical reaction taking place at the interfaces of different phases [31]. Firstly, in the experiment, oleic acid, NaOH and ethanol were put together to form two phases including the liquid phase of the excess oleic acid and ethanol, and the solid phase of sodium oleate [29,30]. Then,  $\text{Zn}(\text{NO}_3)_2$  solution was added into the above mixture, in which a third phase formed (the solution phase). When the mixture was stirred intensely, a phase transfer process of  $\text{Zn}^{2+}$  ions occurred spontaneously across the interface of the sodium oleate and the water/ethanol solution based on ion exchange, which led to the formation of  $(\text{RCOO}^-)_n\text{Zn}^{2+}$ . Finally,  $\text{PO}_4^{3-}$  ions were added into this system, and in the solution phase  $\text{PO}_4^{3-}$  reacted with some of  $\text{Zn}^{2+}$  ions to form zinc phosphate nuclei. The zinc phosphate nuclei were capped by oleic acid on the surface because of the intense interaction between  $\text{Zn}^{2+}$  and the polar groups from oleic acid. In this process, NaOH was used to convert the oleic acid to sodium oleate that was the main solid phase. Obviously, the NaOH addition has an important effect on the content of oleic acid in the reaction. Under the special condition, the zinc phosphate nuclei would grow and self-assemble to sphere shape. Based on the above analysis, a schematic illustration showing the possible growth process of the microspheres is given in Fig. 5.



**Fig. 4** SEM images of as-obtained samples prepared at different NaOH contents: (a) 0.20 g; (b) 0.25 g; (c) 0.30 g; (e) 0.40 g; (f) 0.45 g; (d) EDX spectrum of samples synthesized with 0.30 g NaOH



**Fig. 5** Illustration for formation process of monodisperse zinc phosphate microspheres

### 3.3 Optical performance

The optical properties of the zinc phosphate products were investigated at room temperature. Figure 6 shows the emission spectra of the zinc phosphate samples with different morphologies by changing the NaOH content. From Fig. 6, it can be seen that all the

as-prepared samples display a broad emission band, and the shape and profile of the emission spectra vary little, but the intensity changes remarkably. The sphere-shaped samples prepared with 0.30 and 0.40 g NaOH have a higher PL intensity than other samples. The reason might be that the spherical morphology is of high packing

densities and low scattering of light [18,32,33]. Taking the sphere-shaped samples prepared with 0.30 g NaOH as an example, the emission and excitation spectra are shown in Fig. 7. The emission spectrum (solid line) displays a strong broad band from 430 to 600 nm with a maximum peak at 467 nm. The corresponding excitation spectrum (dashed line) consists of a strong broad range from 300 to 420 nm centered at 400 nm. The feature of long-wavelength UV light excitation is seldom found in the conventional zinc phosphate luminescent materials, which are doped with luminescent centers and excited by less than 400 nm UV light for operation. The chromaticity coordinates (CIE) of the samples are  $x=0.183$ ,  $y=0.276$ , which locates in the blue region (inset in Fig. 7).

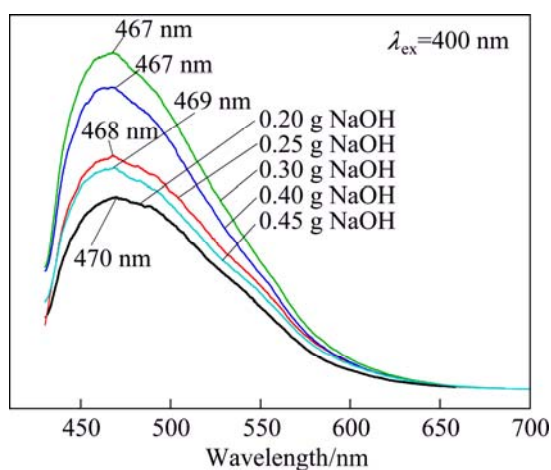


**Fig. 6** PL spectra of as-obtained samples prepared with different contents of NaOH

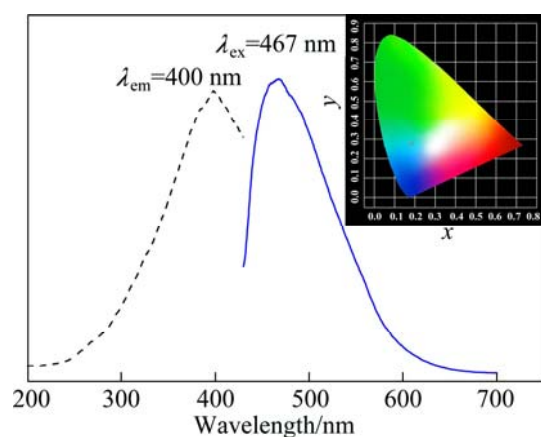


**Fig. 7** PL excitation (dash line) and emission spectrum (solid line) of as-obtained samples synthesized with 0.30 g NaOH (Inset: CIE chromaticity diagram evaluated from emission spectrum)

There are no any other activated ions introduced in this synthesized process, so the observed luminescent property from the zinc phosphate samples can be ascribed to the self-activated luminescence. So far, there

is no report about the property of the self-activated luminescent zinc phosphate phosphor. Considering the FT-IR and EDX results, it can be concluded that a certain level of carbon-related impurities or defects exist in the products. The possible reason is that in the formation process of zinc phosphate samples the adsorbed oleic acid molecules can introduce some carbons to the surfaces of the samples, which will cause some impurities or defects in the crystals. Moreover, the broad feature of emission band (shown in Figs. 6 and 7) indicates that there are a large number of impurities or defects in the products. Finally, the decay curve for the luminescence of the zinc phosphate samples is shown in Fig. 8, which gives the lifetimes of  $t_1$  (5.146 ns) and  $t_2$  (0.726 ns). The short lifetimes further prove that their luminescence may originate from impurities or defects in the zinc phosphate samples [18,25,34].

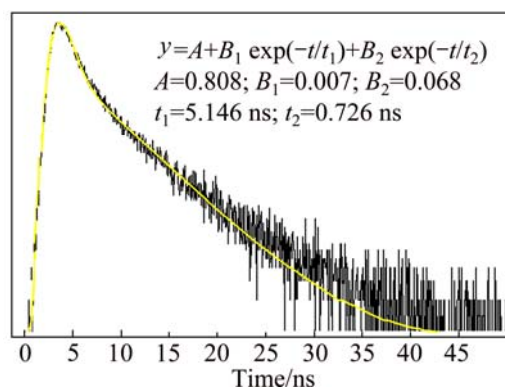


**Fig. 8** Decay curves for luminescence of zinc phosphate samples prepared with 0.3 g NaOH

## 4 Conclusions

- 1) The synthesized zinc phosphate powders are highly crystalline and well-dispersed spherical shapes with uniform size in the range of 3–5  $\mu\text{m}$ .
- 2) Oleic acid is essential in the formation of the monodisperse microspheres. The NaOH content has an obvious impact on the morphology of zinc phosphate products.
- 3) The samples show a novel self-activated luminescent phenomenon, which exhibit a strong emission peak at 467 nm under the long-wavelength UV excitation. The possible luminescent mechanism may be ascribed to carbon-related impurities or defects in the samples.

## Acknowledgements

The authors are grateful to You-yi ZHU, Wen-li LUO, Qing-xia LIN and Qing-feng HOU at PetroChina Exploration & Development Research Institute for their keen interest and kindly acknowledge for providing SEM instrumentation.

## References

- [1] ALIVISATOS A P. Semiconductor clusters, nanocrystals, and quantum dots [J]. *Science*, 1996, 271(5251): 933–937.
- [2] SONG Y J, GARCIA R M, DORIN R M, WANG H R, QIU Y, COKER E N, STEEN W A, MILLER J E, SHELNUTT J A. Synthesis of platinum nanowire networks using a soft template [J]. *Nano Letters*, 2007, 7(12): 3650–3655.
- [3] XIU Zhi-liang, LÜ Meng-kai, ZHOU Guang-jun, GU Feng, ZHANG Hai-ping, XU Dong, YUAN Duo-rong. A facile soft template synthesis and characterization of PbHAsO<sub>4</sub> nanocrystals [J]. *Materials Research Bulletin*, 2004, 39(13): 2019–2023.
- [4] JIANG Jiu-xin, LIU Jie, LIU Chang, ZHANG Gao-wen, GONG Xing-hou, LIU Jia-ning. Roles of oleic acid during micropore dispersing preparation of nano-calcium carbonate particles [J]. *Applied Surface Science*, 2011, 257(16): 7047–7053.
- [5] NIU Na, YANG Piao-ping, WANG Wen-xin, HE Fei, GAI Shi-li, WANG Dong, LIN Jun. Solvothermal synthesis of SrMoO<sub>4</sub>:Ln (Ln=Eu<sup>3+</sup>, Tb<sup>3+</sup>, Dy<sup>3+</sup>) nanoparticles and its photoluminescence properties at room temperature [J]. *Materials Research Bulletin*, 2011, 46(3): 333–339.
- [6] LI Li, CAO Xue-qin, ZHANG You, GUO Chang-xin. Synthesis and upconversion luminescence of Lu<sub>2</sub>O<sub>3</sub>:Yb<sup>3+</sup>,Tm<sup>3+</sup> nanocrystals [J]. *Transactions of Nonferrous Metals Society of China*, 2012, 22(2): 373–379.
- [7] FERHI M, HORCHANI-NAIFER K F, RID M. Hydrothermal synthesis and photoluminescence of the monophosphate LaPO<sub>4</sub>:Eu(5%) [J]. *Journal of Luminescence*, 2008, 128(11): 1777–1782.
- [8] GAO Rui, QIAN Dong, LI Wei. Sol–gel synthesis and photoluminescence of LaPO<sub>4</sub>:Eu<sup>3+</sup> nanorods [J]. *Transactions of Nonferrous Metals Society of China*, 2010, 20(3): 432–436.
- [9] SMITH A L. Luminescence of three forms of zinc orthophosphate:Mn [J]. *Journal of the Electrochemical Society*, 1951, 98(9): 363–368.
- [10] WANG Jing, WANG Shu-bin, SU Qiang. Synthesis, photoluminescence and thermostimulated-luminescence properties of novel red long-lasting phosphorescent materials β-Zn<sub>3</sub>(PO<sub>4</sub>)<sub>2</sub>:Mn<sup>2+</sup>, M<sup>3+</sup> (M=Al and Ga) [J]. *Journal of Materials Chemistry*, 2004, 14(16): 2569–2574.
- [11] MAUREL C, CARDINAL T, BELLEC M, CANIONI L, BOUSQUET B, TREGUER M, VIDEAU J J, CHOI J, RICHARDSON M. Luminescence properties of silver zinc phosphate glasses following different irradiations [J]. *Journal of Luminescence*, 2009, 129(12): 1514–1518.
- [12] GU Jian-feng, YAN Bing. Controlled synthesis and photoluminescence of Zn<sub>3</sub>(PO<sub>4</sub>)<sub>2</sub>:Eu<sup>3+</sup> nanocrystal via hydrothermal process [J]. *Journal of Optoelectronics and Advanced Materials*, 2008, 10(2): 405–409.
- [13] SHEN Wei-ying, LIN Jun, YU Min, HAN Xiu-mei. Citrate-gel synthesis and luminescent properties of α-Zn<sub>3</sub>(PO<sub>4</sub>)<sub>2</sub> doped with Eu<sup>3+</sup> [J]. *Journal of Rare Earths*, 2004, 22(1): 87–90.
- [14] MA Chong-geng, JIANG Sha, ZHOU Xian-ju. Energy transfer from Ce<sup>3+</sup> to Tb<sup>3+</sup> and Eu<sup>3+</sup> in zinc phosphate glasses [J]. *Journal of Rare Earths*, 2010, 28(1): 40–42.
- [15] LIU Yin-yao, ZOU Zhao-song, LIANG Xiao-luan, WANG Shu-fen, XING Zhong-wen, CHEN Guo-rong. Energy transfer and photoluminescence of zinc phosphate glasses co-doped with Tb<sup>3+</sup> and Mn<sup>2+</sup> [J]. *Journal of the American Ceramic Society*, 2010, 93(7): 1891–1893.
- [16] PANG Ran, LI Cheng-yu, JIANG Li-hong, SU Qiang. Blue long lasting phosphorescence of Tm<sup>3+</sup> in zinc pyrophosphate phosphor [J]. *Journal of Alloys and Compounds*, 2009, 471(1–2): 364–367.
- [17] GREEN W H, LE K P, GREY J, AU T T, SAILOR M J. White phosphors from a silicate-carboxylate sol–gel precursor that lack metal activator ions [J]. *Science*, 1997, 276(5320): 1826–1828.
- [18] ZHANG Cui-miao, YANG Jun, QUAN Ze-wei, YANG Piao-ping, LI Chun-xia, HOU Zhi-yao, LIN Jun. Hydroxyapatite nano- and microcrystals with multiform morphologies: Controllable synthesis and luminescence properties [J]. *Crystal Growth & Design*, 2009, 9(6): 2725–2733.
- [19] ANGELOV S, STOYANOVA R, DAFINOVA R, KABASANOV K. Luminescence and EPR studies on strontium carbonate obtained by thermal decomposition of strontium oxalate [J]. *Journal of Physics and Chemistry of Solids*, 1986, 47(4): 409–412.
- [20] JAKOB A M, SCHMEDAKE T A. A novel approach to monodisperse, luminescent silica spheres [J]. *Chemistry of Materials*, 2006, 18(14): 3173–3175.
- [21] ZHANG Xiao-ming, QUAN Ze-wei, YANG Jun, YANG Piao-ping, LIAN Hong-zhou, LIN Jun. Solvothermal synthesis of well-dispersed NaMgF<sub>3</sub> nanocrystals and their optical properties [J]. *Journal of Colloid and Interface Science*, 2009, 329(1): 103–106.
- [22] LIN Cui-kun, ZHANG Cui-miao, LIN Jun. Sol–gel derived Y<sub>2</sub>O<sub>3</sub> as an efficient bluish-white phosphor without metal activator ions [J]. *Journal of Luminescence*, 2009, 129(12): 1469–1474.
- [23] JUNG S H, OH E, LIM H, SHIM D S, CHO S, LEE K H, JEONG S H. Shape-selective fabrication of zinc phosphate hexagonal bipyramids via a disodium phosphate-assisted sonochemical route [J]. *Crystal Growth & Design*, 2009, 9(8): 3544–3547.
- [24] BRONSTEIN L M, HUANG X L, RETRUM J, SCHMUCKER A, PINK M, STEIN B D, DRAGNEA B. Influence of iron oleate complex structure on iron oxide nanoparticle formation [J]. *Chemistry of Materials*, 2007, 19(15): 3624–3632.
- [25] ZHANG Xiao-ming, QUAN Ze-wei, YANG Jun, YANG Piao-ping, LIAN Hong-zhou, LIN Jun. Solvothermal synthesis of well-dispersed MF<sub>2</sub> (M=Ca, Sr, Ba) nanocrystals and their optical properties [J]. *Nanotechnology*, 2008, 19(7): 075603-1-8.
- [26] HE Qian-jun, HUANG Zhi-liang, LIU Yu, CHEN Wei, XU Tao. Template-directed one-step synthesis of flowerlike porous carbonated hydroxyapatite spheres [J]. *Materials Letters*, 2007, 61(1): 141–143.
- [27] SALARIAN M, SOLATI-HASHJIN M, SHAFIEI S S, SALARIAN R, NEMATI Z A. Template-directed hydrothermal synthesis of dandelion-like hydroxyapatite in the presence of cetyltrimethylammonium bromide and polyethylene glycol [J]. *Ceramics International*, 2009, 35(7): 2563–2569.
- [28] CHEN Yin-Xia, JI Xian-bing, WANG Xiao-bo. Facile synthesis and characterization of hydrophobic vaterite CaCO<sub>3</sub> with novel spike-like morphology via a solution route [J]. *Materials Letters*, 2010, 64(20): 2184–2187.
- [29] LIU Jun-feng, LI Ya-dong. General synthesis of colloidal rare earth orthovanadate nanocrystals [J]. *Journal of Materials Chemistry*, 2007, 17(18): 1797–1803.
- [30] LIANG Xin, WANG Xun, ZHUANG Jing, CHEN Yong-tao, WANG Ding-sheng, LI Ya-dong. Synthesis of nearly monodisperse iron oxide and oxyhydroxide nanocrystals [J]. *Advanced Functional Materials*, 2006, 16(14): 1805–1813.
- [31] WANG Xun, ZHUANG Jing, PENG Qing, LI Ya-dong. A general strategy for nanocrystal synthesis [J]. *Nature*, 2005, 437(7055): 121–124.
- [32] VECHT A, GIBBONS C, DAVIES D, JING X P, MARSH P, IRELAND T, SILVER J, NEWPORT A, BARBER D. Engineering phosphors for field emission displays [J]. *Journal of Vacuum Science & Technology B*, 1999, 17(2): 750–757.
- [33] WAKEFIELD G, HOLLAND E, DOBSON P J, HUTCHINSON J L. Luminescence properties of nanocrystalline Y<sub>2</sub>O<sub>3</sub>:Eu [J]. *Advanced Materials*, 2001, 13(20): 1557–1560.
- [34] ZHANG Cui-miao, CHENG Zi-yong, YANG Piao-ping, XU Zhen-he, PENG Chong, LI Guo-gang, LIN Jun. Architectures of strontium hydroxyapatite microspheres: Solvothermal synthesis and luminescence properties [J]. *Langmuir*, 2009, 25(23): 13591–13598.

## 磷酸锌微球的制备及光学性能

宁张磊, 李文军, 孙长艳, 车平, 常志东

北京科技大学 化学与生物工程学院, 北京 100083

**摘要:** 在油酸存在下, 采用简单的溶剂热方法制备单分散的磷酸锌微米球。通过 X 射线粉末衍射、傅里叶红外光谱、扫描电子显微镜、能谱等方法对磷酸锌产品的结构和形貌进行表征。实验结果表明, 制备的磷酸锌产品结晶性良好, 并且产品的形貌可以通过油酸添加量和氢氧化钠的加入量实现有效的控制。该产品具有自发光性能, 在 400 nm 长波紫外光的激发下, 可以发射出明亮的蓝光。推测可能的发光机理为与碳相关的表面杂质或者缺陷所致。

**关键词:** 磷酸锌; 油酸; 化学合成; 光学性能; 发光性能

(Edited by Wei-ping CHEN)